Oscillation Mode Identification in Converter-based Offshore System using Dynamic Mode Decomposition

Castrillón-Franco, C.; Rueda-Torres, J. L.; Narayanan, N.; Messina, A. R.

DOI
10.1109/IECON58223.2025.11221794

Publication date
2025

Document Version
Final published version

Published in
Proceedings of the IECON 2025 – 51st Annual Conference of the IEEE Industrial Electronics Society

Citation (APA)
Castrillón-Franco, C., Rueda-Torres, J. L., Narayanan, N., & Messina, A. R. (2025). Oscillation Mode Identification in Converter-based Offshore System using Dynamic Mode Decomposition. In *Proceedings of the IECON 2025 – 51st Annual Conference of the IEEE Industrial Electronics Society* (IECON Proceedings (Industrial Electronics Conference)). IEEE. https://doi.org/10.1109/IECON58223.2025.11221794

Oscillation Mode Identification in Converter-based Offshore System using Dynamic Mode Decomposition

Camila Castrillón-Franco, José Luis Rueda-Torres, Nakul Narayanan
Intelligent Electrical Power Grids
Delft University of Technology
Delft, The Netherlands
email: mcastrillonfra@tudelft.nl, j.l.ruedatorres@tudelft.nl, k.narayanankuruveettil@tudelft.nl

Arturo Román Messina
Graduate Studies Program in Electrical Engineering
Cinvestav
Guadalajara, Mexico
email: arturo.roman@cinvestav.mx

IECON 2025 – 51st Annual Conference of the IEEE Industrial Electronics Society | 979-8-3315-9681-1/25/$31.00 ©2025 IEEE | DOI: 10.1109/IECON58223.2025.11221794

***Abstract*—Converter-interfaced renewable generation predominates in the development of new power system architectures, particularly in offshore systems. The increase of such multi-converter systems leads to the introduction of a new interaction among the different elements of the system and, therefore, new dynamic phenomena. Such phenomenon is subsynchronous and super-synchronous oscillations (SSO) which result, among other causes, from the interaction of converters with weak networks, such as offshore power systems. Various factors, including the challenge of obtaining analytical models from converter-based generation manufacturers and analysing system measurements during planning and operations, necessitate effective measurement-based methods for the swift and numerically trustworthy identification of various characteristics of SSO. Therefore, this paper analyses the advantages and disadvantages of the Dynamic Mode Decomposition method for identifying SSO. The theoretical background of the technique and the application algorithm are presented. The method is first applied to several synthetic signals exhibiting subsynchronous and supersynchronous modes under various conditions, including noise and different time windows. Then, a converted-based resource connected to an infinite bus is presented, and the method is applied to a group of recorded signals from this system under an external perturbation. This method is proposed as an alternative for analysing SSO in converted-based systems due to its ability to assess non-linear systems and its robustness against noise.**

***Index Terms*—Converter-based resource system, Dynamic Mode Decomposition, Koopman Modes, Wind Generator, Subsynchronous oscillations.**

I. Introduction

The growing integration of renewable energy sources and various devices based on power electronic converters has altered the dynamics of power networks, rendering them susceptible to oscillations across a broad frequency spectrum. According to [1], more than 1,200 oscillatory modes have been identified across several test cases in a simulation model of a wind farm connected via HVDC to the main network. Most of the events documented in the literature occur within 1 Hz to 10 Hz and significantly impact the power system, leading to outages and damage to surrounding elements and loads.

Subsynchronous and super-synchronous oscillations (SSO) are events linked to converter-interfaced generation within the 1 to 100 Hz frequency range. The oscillation frequency may be below or above the fundamental frequency (50 Hz or 60 Hz), but it does not encompass electromechanical oscillations, which occur at frequencies between 0.1 and 2 Hz. Various mechanisms identified could lead to these oscillations in the recorded events, including interactions with series capacitors and unstable controls interacting with a weak grid (low short-circuit ratio (SCR)) [2].

Oscillation events associated with converter-interfaced generation are documented in several documents [2], [3]. These events can generally be caused by series compensation of transmission lines or interactions between converters in weak grids. According to [2], the first reported event of wind SSO caused by low SCR might be the Texas event of 2011, where an outage of a 138 kV line left a WPP connected through a weak 69 kV line, resulting in 4 HZ oscillations. According to ERCOT's stability studies, the causes of these oscillations were weak system conditions and improper tuning of the wind turbine voltage controller. The same document analyses a notable example of the interactions between type 4 wind turbines and a weak grid; the event in question was recorded in 2014 in Xinjiang, China [4].

To identify and assess these types of oscillations, different strategies have been implemented in the literature, such as impedance scanning [5], detailed EMT simulations [6], [7] and Small Signal Analysis [8]–[10]. The literature has demonstrated how these methods can successfully identify oscillations. However, the analytical model of the system is required to apply these methods. In the case of impedance scanning, the results depend on the point of the system where the method is implemented.

The research work shown in this paper has received funding from TenneT TSO B.V within the research project on Adaptive identification and mitigation of variable oscillatory phenomena in weakening networks - FORBES. It reflects only the authors views, and the aforesaid organization is not responsible for any use that may be made of the paper's content.

For the reasons above, measurement-based methods have been proposed. In the frequency domain, the most implemented method is the Fourier Fast Transform, and in the time domain, the Prony methodology is widely used as a benchmark to compare other approaches, where data samples are fitted to an exponential model [11]. Other approaches are the Eigensystem Realization Algorithm (ERA), matrix pencil, and the estimation of signal parameters via the rotational invariance technique (ESPRIT) [12]. These methods have been applied in studying different phenomena, such as electromechanical oscillations. However, these methods are sensitive to noise, present a high error rate in identifying damping, and require some inputs, such as the order of the identified system.

Due to the lack of studies analysing the performance of measurement-based methods in identifying SSO, this paper investigates the advantages and drawbacks of using the Dynamic Mode Decomposition method, a numerical method that approximates the Koopman functions of a given dataset [13]. The primary contribution of this research is the application of two measurement-based methods to identify the principal parameters of SSO under various conditions, including the presence of noise and parameter changes. Additionally, the methods are applied to recorded data from real-time simulation to study the performance in applying the DMD method.

The remaining part of the paper is organized as follows: Section II presents the DMD method's theoretical background and the representation of subsynchronous and supersynchronous oscillations. Section III summarizes the selected case studies and simulation results, and Section IV concludes the main findings of the present research.

II. Representation and Identification of SSO Modes

A. Subsynchronous oscillation Modelling

The SSO can be modelled as the sum of a fundamental component and a pair of frequency-coupled subsynchronous and super-synchronous components, denoted by $y(t)$ as,

$$y(t) = x_{f0}(t) + x_{sub}(t) + x_{sup}(t) \tag{1}$$

Where:

$$\begin{aligned} x_{f0}(t) &= A_0 cos(2\pi f_0 + \varphi_0) \\ x_{sub}(t) &= A_{sub} e^{\zeta_{sub} t} cos(2\pi f_{sub} + \varphi_{sub}) \\ x_{sup}(t) &= A_{sup} e^{\zeta_{sup} t} cos(2\pi f_{sup} + \varphi_{sup}) \end{aligned}$$

In the previous equations, A_n represents the amplitude, f_n the frequency, ζ_n the damping ratio and φ_n the phase of each component. The subscripts $0, sub, sup$ represent the variables of the fundamental, synchronous and super-synchronous components, respectively.

In the SSOs, the frequencies of the modes satisfy that $f_{sub} + f_{sup} = 2f_0$. In SSOs caused by converter-based generation interaction, the coupling effects are induced by the dq/abc transformation inherent in the converter controllers [14].

B. Dynamic Mode Decomposition

Dynamic Mode Decomposition (DMD) [15] is a measurement-based method used to identify the frequency and damping of oscillatory modes present in a set of recorded signals. This numerical method approximates Koopman functions using a set of data snapshots that are evenly spaced.

Consider a discrete system in the form:

$$x_{k+1} = f(x_k), k = 0, 1, 2, ...N \tag{2}$$

where k is an integer index. Also, consider a scalar-valued function in the form $g(x) : M \to \mathbb{R}$. A Koopman operator, V, is a linear operator that maps g into a new function:

$$Vg(x) = g(f(x)) \tag{3}$$

The objective of the Koopman operators is to study the dynamic characteristics of the system under study; for this reason, it is required to obtain the eigenspectrum of V. Assume that ϕ_i and λ_j, denote the eigenfunctions and eigenvalues of the Koopman operators and are given by:

$$V\phi_j(x) = \lambda_j \phi_j(x), \quad j = 1, 2, ... \tag{4}$$

In practice, there is an interest in function $g(x) = [g_1 \quad (x) \quad g_2(x) \quad ... \quad g_p(x)] = M \to p$ with $p < N$. Assuming that each of the components of lie within the span of the eigenfunctions the time evolution of the functions the time evolution of the functions can be expanded as:

$$g(x) = \sum_{j=1}^{\infty} \phi_j v_j \tag{5}$$

and

$$x_k = g(x_k) = \sum_{j=1}^{\infty} V^k \phi_j(x_0) v_j = \sum_{j=1}^{\infty} \lambda j^k \phi_j(x_0) v_j \tag{6}$$

The equation 6 indicates that the observables (a measurement of the state) $g(x_k)$ are decomposed into vector coefficients v_j, called Koopman modes, and they have equivalents eigenvalues λj.

However, to obtain the Koopman modes in practical applications, a data-driven method is required because the Koopman operator is a linear operator of infinite dimensions. For this reason, Dynamic Mode Decomposition (DMD) is used since DMD approximates the Koopman operator in a finite-dimensional subspace for practical computation.

1) Dynamic Mode Decomposition Algorithm: The step-by-step procedure for applying the identification method is presented as follows:

- Obtain the measurements of the system in which the oscillatory modes will be identified as $x(v_j, t_i), j = 1, ..., m, i = 1, 2, ...l, ..., N$ where v_j is the measurement point, and t_i is the time at which the observations were made. Then arrange them in the form X_1^N:

$$X_1^N = \begin{bmatrix} x(v_1,t_1) \cdots x(v_1,t_l) \cdots x(v_1,t_N) \\ \vdots \qquad\qquad \vdots \qquad\qquad \vdots \\ x(v_m,t_1) \cdots x(v_m,t_l) \cdots x(v_m,t_N) \end{bmatrix} \tag{7}$$

The lth column is the observation sequence x_l.

- Pre-processing of signals is conducted in two stages. The first stage involves filtering the signals to eliminate noise and the second step in signal preprocessing is to apply a detrending technique to highlight the oscillation characteristics in the signals
- The implementation of the DMD algorithm begins by arranging the signals according to the Krylov sequence. Assuming that the data sequences are generated by a discrete-time linear dynamical system described as:

$$x_{i+1} = Ax_i, \quad i = 1, .., N-1 \tag{8}$$

The sequences could be presented as:

$$X_1^N = \begin{bmatrix} x_1 & Ax_1 & A^2x_1 & \cdots & A^{N-1}x_1 \end{bmatrix} = \begin{bmatrix} x_1 & \cdots & x_N \end{bmatrix} \tag{9}$$

$$X_1^{N-1} = \begin{bmatrix} x_1 & Ax_1 & \cdots & A^{N-2}x_1 \end{bmatrix} = \begin{bmatrix} x_1 & \cdots & x_{N-1} \end{bmatrix} \tag{10}$$

$$X_2^N = \begin{bmatrix} Ax_1 & A^2x_1 & \cdots & A^{N-1}x_1 \end{bmatrix} = \begin{bmatrix} x_2 & \cdots & x_N \end{bmatrix} \tag{11}$$

- Compute the QR decomposition of the vector X_1^{N-1}.
- Obtain the Singular value decomposition of the obtained matrix in the previous step.

$$S = U\Sigma W^T \tag{12}$$

- Form the matrix $S = U^T X_2^N W \Sigma^{-1}$ and,
- Compute the eigenvalues λ_i and y_i eigenvectors of S. The ith DMD eigenvalue is λ_i and the ith DMD mode is the Uy_i.

III. Cases Studies and Simulation Results

To assess the performance and accuracy of the DMD method in SSO identification, synthetic signals are first generated and modified to test the method's robustness under varying conditions, including noise and changes in oscillation parameters. The method is then applied to identify the modes in the response of an infinite bus system to an external disturbance. Additionally, the Prony method is used to compare the results obtained, as it is a widely known method proposed for these kinds of applications.

The Prony method assumes that a signal $y(t)$ can be expressed as a linear combination of n exponentially damped sinusoids:

$$y(t) = \sum_{i=1}^{n} c_i e^{\lambda_i t} \tag{13}$$

Where c_i is the amplitude of the i-th component and λ_i is the frequency and damping of each mode. The Prony algorithm implemented in the Matlab-based Dynamic System Identification toolbox (DSI Toolbox version 3.1.8) by NASPI [16] has been used in this paper for SSO identification.

A. Synthetic Signals

1) Application of DMD in multi-mode synthetic signal: The DMD's performance is assessed when the signal consists of the fundamental component at 50 Hz and two oscillatory modes, with varying parameters for each mode.

For the fundamental component the used values are A_1 = 0.05, f_1 = 50 Hz, φ_1 = -1.3.

Four cases presented in Table I were used to test different conditions. Case 1 includes two modes with a critical damping ratio; Case 2 features a mode with a critical damping ratio and one unstable mode. The damping ratios in case 3 are the same as in case 1, but one of the modes has a lower amplitude and, therefore, a lower power. Case 4 has two modes with frequencies closer to the nominal frequency of 50 Hz.

TABLE I
Subsynchronous and Super-Synchronous Oscillation Parameters

Case	Sub-SO component	Sup-SO component
Case 1	A_{sub} = 0.08, ζ_{sub} = 0.01 s^{-1} f_1 = 15 Hz, φ_1 = 0.75	A_{sup} = 0.15, ζ_{sup} = 0.009 s^{-1} f_1 = 85 Hz, φ_1 = 2
Case 2	A_{sub} = 0.08, ζ_{sub} = 0.01 s^{-1} f_1 = 15 Hz, φ_1 = 0.75	A_{sup} = 0.15, ζ_{sup} = -0.008 s^{-1} f_1 = 85 Hz, φ_1 = 2
Case 3	A_{sub} = 0.008, ζ_{sub} = 0.01 s^{-1} f_1 = 15 Hz, φ_1 = 0.75	A_{sup} = 0.15, ζ_{sup} = 0.009 s^{-1} f_1 = 85 Hz, φ_1 = 2
Case 4	A_{sub} = 0.08, ζ_{sub} = 0.01 s^{-1} f_1 = 48 Hz, φ_1 = 0.75	A_{sup} = 0.15, ζ_{sup} = 0.009 s^{-1} f_1 = 52 Hz, φ_1 = 2

The synthetic signals with the previously described parameters are presented in Figure 1.

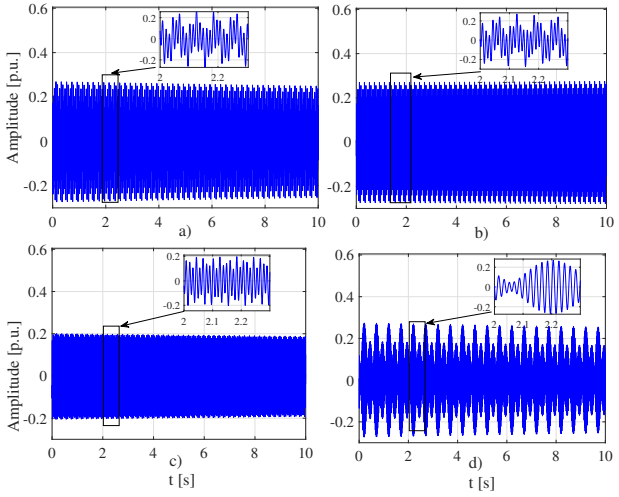

Fig. 1. Synthetic signals for DMD analysis with subsynchronous and supersynchronous modes and noise a) case 1, b) case 2, c) case 3, d) case 4

The identification results are presented in Table II. With both methods, the frequencies identified are highly accurate and correspond to the theoretical values. However, damping values exhibit a maximum percentage error of 15% in case 4 when the frequencies are closer to the principal component.

2) Sensitivity to different noise levels: The influence of noise on the identification process using the DMD method is evaluated. To this aim, the synthetic signal described in

TABLE II
SUBSYNCHRONOUS AND SUPER-SYNCHRONOUS IDENTIFIED PARAMETERS USING THE DMD METHOD

Cases	Prony				DMD			
	ζ_{id} [%]	$\varepsilon_{\zeta_{id}}$ [%]	f_{id} [Hz]	$\varepsilon_{f_{id}}$ [%]	ζ_{id} [%]	$\varepsilon_{\zeta_{id}}$ [%]	f_{id} [Hz]	$\varepsilon_{f_{id}}$ [%]
Case 1	0.0106	0.097	15.000	0.000	0.0106	0.097	15.0000	0.000
	0.0016	5.054	85.000	0.000	0.0016	5.054	85.0000	0.000
Case 2	0.0106	0.097	15.000	0.000	0.0106	0.097	15.0000	0.000
	-0.0014	6.538	85.000	0.000	-0.0015	0.138	85.0000	0.000
Case 3	0.0106	0.097	15.000	0.000	0.0106	0.097	15.0000	0.000
	0.0016	6.814	85.000	0.000	0.0014	6.538	85.0000	0.000
Case 4	0.0033	0.474	48.000	0.000	0.0033	0.474	48.0000	0.000
	0.0027	10.270	52.000	0.000	0.0028	14.354	52.0000	0.000

equation 1 is altered by adding a noise component as indicated in equation 14:

$$y(t) = x(t) + n(t) \tag{14}$$

where $y(t)$ is the noisy signal, $x(t)$ is the original signal and $n(t)$ is the noise. The noise $n(t)$ has a Gaussian Distribution, and each sample is defined from a Gaussian (normal) distribution:

$$n(t) \sim N(0, \sigma^2) \tag{15}$$

Where 0 is the mean, and σ^2 is the variance related to the noise power and is defined in the form:

$$\sigma = \sqrt{\frac{A^2_{signal}}{10^{\frac{SNR}{10}}}} \tag{16}$$

Where A_{signal} is the signal amplitude and SNR is Signal-to-Noise Ratio.,

In this sensitivity, the case 4 parameters are used, and the range variation of SNR is from 20 dB to 50 dB according to the noise levels reported in the literature [17]. The signals with an SNR of 20 dB and 50 dB are presented in figure 2

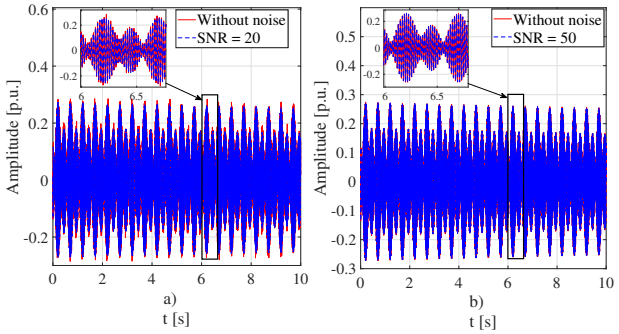

Fig. 2. Synthetic signals for DMD analysis with subsynchronous and super-synchronous modes and noise a) SNR = 20 dB 1, b) SNR = 50 dB

Table III presents the identification results obtained with both methods. Each SNR value is associated with two rows, corresponding to the parameters of the two modes present in the signal. As expected, the frequency was well identified with both methods, although a higher percentage error was obtained with the Prony method at lower SNR values. Additionally, a more accurate damping identification was achieved at higher noise levels using the DMD than with the Prony method. However, the percentage error varies according to the settings

TABLE III
IDENTIFIED OSCILLATION PARAMETERS AND DEVIATION FROM THEORETICAL VALUES IN SYNTHETIC SIGNAL WITH ADDED NOISE.

SNR [dB]	Prony				DMD			
	ζ_{id} [%]	$\varepsilon_{\zeta_{id}}$ [%]	f_{id} [Hz]	$\varepsilon_{f_{id}}$ [%]	ζ_{id} [%]	$\varepsilon_{\zeta_{id}}$ [%]	f_{id} [Hz]	$\varepsilon_{f_{id}}$ [%]
20	0.0839	3326.535	51.9561	0.084	0.00249	1.693	52.001	0.002
	0.2811	8377.776	48.1465	0.305	0.00340	2.542	47.9981	0.004
25	0.0750	2963.053	51.9940	0.012	0.00261	6.594	52.0002	0.000
	0.2444	7270.930	48.0499	0.104	0.00387	16.716	47.9997	0.001
30	0.0298	1117.053	51.9999	0.000	0.00299	22.114	51.9999	0.000
	0.1202	3525.147	47.9894	0.022	0.00362	9.177	47.9999	0.000
35	0.0141	475.854	52.0003	0.001	0.00277	13.129	51.9999	0.000
	0.0414	1148.595	47.9951	0.010	0.00368	10.986	47.9999	0.000
40	0.0053	116.456	52.0003	0.001	0.00290	18.438	52.0000	0.000
	0.0163	391.596	47.9989	0.002	0.00366	10.383	47.9998	0.000
45	0.0036	47.027	51.9998	0.000	0.00298	21.705	52.0000	0.000
	0.0063	90.004	47.9993	0.001	0.00390	17.621	47.9999	0.000
50	0.0031	26.606	52.0003	0.001	0.00291	18.846	52.0000	0.000
	0.0048	44.765	47.9997	0.001	0.00348	4.954	48.0000	0.000

used to apply the DMD method, such as the number of input signals.

Considering that measurements from different sources, such as PMUs, have noise with a non-Gaussian distribution, a sensitivity analysis is performed by adding a Laplacian distribution, which has been considered in other studies to model the type of noise present in PMUs [18]. In this sensitivity analysis, the SNR of 20 dB and 50 dB, which are the maximum and minimum values used in the previous sensitivity analysis, are assessed and presented in Table IV. Although it has a higher error rate for signals with Gaussian noise, the DMD method exhibits a lower error rate than the Prony method.

TABLE IV
IDENTIFIED OSCILLATION PARAMETERS FROM THEORETICAL VALUES IN SYNTHETIC SIGNAL WITH ADDED NON-GAUSSIAN NOISE.

SNR [dB]	Prony				DMD			
	ζ_{id} [%]	$\varepsilon_{\zeta_{id}}$ [%]	f_{id} [Hz]	$\varepsilon_{f_{id}}$ [%]	ζ_{id} [%]	$\varepsilon_{\zeta_{id}}$ [%]	f_{id} [Hz]	$\varepsilon_{f_{id}}$ [%]
20	0.7240	25757	51.9572	0.0823	0.0031	10.7143	52.0004	0.0007
	3.0190	91385	48.1451	0.3023	0.0068	106.0606	47.9985	0.0087
50	0.0048	74.4286	51.9998	0.0003	0.0027	3.5714	52.0001	0.0001
	0.0030	9.0909	48.0000	0.0000	0.0033	0.0000	47.9996	0.0008

3) Sensitivity to changes in frequency and damping: Finally, the impact of changes in the oscillation mode parameters and the time windows is analysed in this section, creating a signal with a subsynchronous and super-synchronous mode. At 10 seconds, the parameters of the oscillations are changed to assess the reliability of the method under parameter changes while also considering the stabilisation time of the variable as it would occur in the operation of a power system. Those parameters are presented in table VI.

TABLE V
SUBSYNCHRONOUS AND SUPERSYNCHRONOUS OSCILLATIONS PARAMETERS

Case	Sub-SO component	Sup-SO component
t >= $10s$	A_{sub} = 0.08, ζ_{sub} = 0.01 s^{-1} f_{sub} = 48 Hz, φ_1 = 0.75	A_{sup} = 0.15, ζ_{sup} = 0.009 s^{-1} f_1 = 52 Hz, φ_1 = 2
t >= $20s$	A_{sub} = 0.08, ζ_{sub} = 0.05 s^{-1} f_1 = 30 Hz, φ_1 = 0.75	A_{sup} = 0.15, ζ_{sup} = 0.03 s^{-1} f_1 = 70 Hz, φ_1 = 2

The signal with the previously described parameters is presented in Figure 3. Figure 3 a) has a time window of 20 seconds for the identification with both methods, and Figure

3 b) is the signal split in two different time windows of 10 seconds each for the identification process.

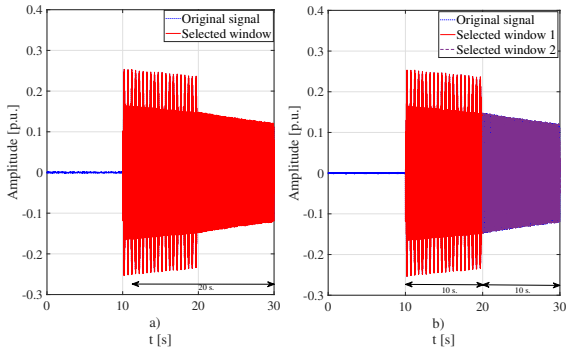

Fig. 3. Synthetic signals to DMD analysis with subsynchronous and super-synchronous modes and changes in frequency and damping

The identification results are presented in Table VI. This analysis shows the importance of an adequate selection of the sampling window because both methods present a quite large damping estimation error. A better result is obtained when a time window is selected where there are no changes in the damping parameters; therefore, signal pre-processing methods are required to select this time window properly.

TABLE VI
IDENTIFIED OSCILLATION PARAMETERS AND DEVIATION FROM THEORETICAL VALUES IN SYNTHETIC SIGNAL WITH ADDED NOISE.

SNR [dB]	Prony				DMD			
	ζ_{id} [%]	$\varepsilon_{\zeta_{id}}$ [%]	f_{id} [Hz]	$\varepsilon_{f_{id}}$ [%]	ζ_{id} [%]	$\varepsilon_{\zeta_{id}}$ [%]	f_{id} [Hz]	$\varepsilon_{f_{id}}$ [%]
Time Window = 20s	0.0254	822.092	52.0002	0.0004	0.03706	1245.384	52.0113	0.0217
	0.0293	783.667	47.9963	0.0077	0.07055	2027.738	47.9798	0.0421
	0.0065	4.705	70.0004	0.0006	0.00781	14.501	70.0006	0.0009
	0.0304	14.605	29.9997	0.0010	0.02996	12.947	30.0008	0.0027
Time Window = 10s	0.0028	1.648	51.9999	0.0002	0.00269	2.345	52.0000	0.0000
	0.0034	2.542	47.9999	0.0002	0.00334	0.732	47.9999	0.0002
	0.0068	0.307	70.0000	0.0000	0.00683	0.133	69.9999	0.0001
	0.0273	2.919	29.9998	0.0007	0.02645	0.286	30.0000	0.0000

B. Data From Simulated SSO Case

To illustrate the use of the DMD method, an example is presented in a system with a grid-following converter connected to an infinite bus. The single-line topology is given in figure 4.

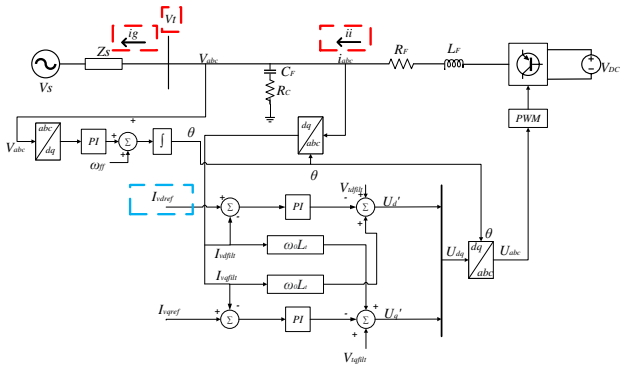

Fig. 4. Grid Following Converter Topology

The system consists of one DC voltage, a two-level AC/DC converter, and a network equivalent with an AC source and equivalent impedance. The Grid-following converter controller is implemented as a current loop in the dq reference frame.

The system parameters are presented in Table VII and implemented in RSCAD for real-time simulation

TABLE VII
PARAMETERS OF GRID FOLLOWING CONVERTER - INFINITE BUS SYSTEM

Parameters	Value
AC Voltage V_s	400 V
Frequency F	50 Hz
Filter Capacitor C_F	5 μF
Filter Resistance R_C	10 Ω
Converter Resistance R_F	1 Ω
Converter Inductance L_F	10 mH
Equivalent impedance Z_S	0.645 + jω0.0067 Ω

To excite an oscillation in the system, a perturbation was applied by changing the direct-axis current reference Id from 0.95 pu to 1 pu at 0.5s; this variable is whitin the blue dotted box in the single-line diagram presented in Figure 4 Then, the recorded signals to apply the identification method are the direct-axis and quadrature-axis of the current converter, voltage and current network; these variables are presented in Figure 4 in the red dotted boxes. The recorded variables are presented in Figure 5.

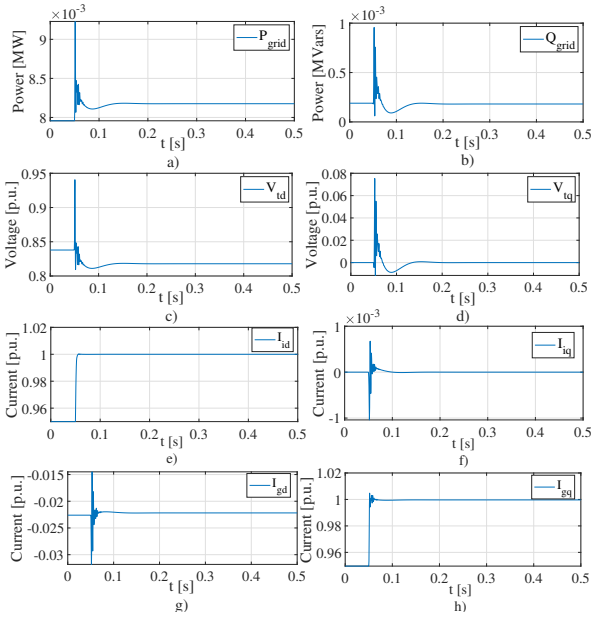

Fig. 5. Recorded signals from a perturbation in the infinite-bus system

The identified mode parameters are presented in Table VIII, which were validated with the eigenvalues obtained from small signal analysis performed in the analytical model. This system presents one subsynchronous oscillatory mod, well-damped, and two super synchronous oscillatory modes in a frequency range that is not harmful to the system operation, according to different experiences presented in the literature. The oscillation parameters obtained through small-signal analysis differ from those identified with data-driven identification methods. Some causes of this difference include that small signal analysis requires the linearisation of a system whose components

behave non-linearly, and some limitations in the time step of the real-time simulation.

TABLE VIII
IDENTIFIED OSCILLATION MODE PARAMETERS IN INFINITE-BUS SYSTEM

SSA		Prony				DMD			
ζ_{th} [%]	f_{th} [Hz]	ζ_{id} [%]	$\varepsilon_{\zeta_{id}}$ [%]	f_{id} [Hz]	$\varepsilon_{f_{id}}$ [%]	ζ_{id} [%]	$\varepsilon_{\zeta_{id}}$ [%]	f_{iden} [Hz]	$\varepsilon_{f_{id}}$ [%]
69.239	**7.772**	**61.79**	**10.758**	**7.54**	**2.985**	**64.521**	**6.814**	**7.29**	**6.202**
7.37	336.6646	11.940	62.008	324.060	3.744	11.791	59.986	325.466	3.326
5.98	447.0999	08.707	45.602	438.900	1.834	8.831	47.676	439.453	1.710

To determine which recorded signals provide the most accurate oscillatory mode identification, the Power Spectral Density (PSD) [19] of the recorded signals was calculated. To obtain the PSD, the Periodogram presented in Figure 6 was obtained. It is possible to conclude that the voltage signals present a higher power at the frequency of interest, allowing a better identification of the modes of interest. This occurs because the oscillations result from the interaction between the voltage control loops of the converters and the AC system.

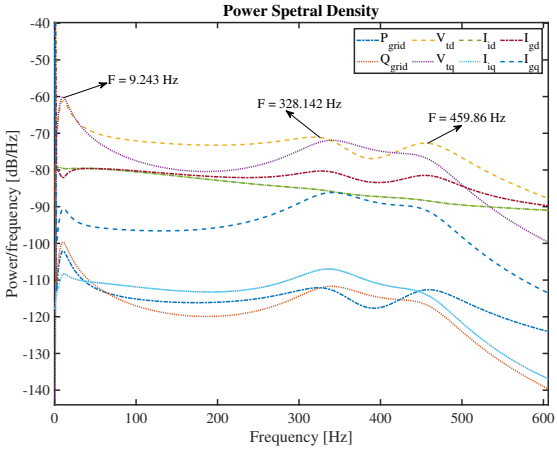

Fig. 6. Power Spectral Density

IV. CONCLUSIONS

This study investigates the implementation of Dynamic Mode Decomposition for detecting subsynchronous and supersynchronous oscillations, emphasizing its strength in identifying dynamic modes in nonlinear systems and its ability to withstand noise. First, the method is applied to synthetic signals. It proved its advantage over a traditional method, such as the Prony method, under different conditions, such as noise, demonstrating more accurate identification at SNR levels below 30 dB, due to its ability to separate the dynamic components of signals from non-linear systems without the requirement of input parameters. However, when there are changes in the frequency and damping of the oscillatory mode along the time window, the method generates an identification value with a higher percentage error than the other method. Therefore, it is important to consider another algorithm to select an appropriate time window. Then, the method is applied to some recorded signals obtained from a Real-time simulation of a converter-based generation connected to an infinite bus system. The results demonstrate the DMD method's capability to identify SSO in a realistic scenario and its comparability to other approaches. The method shows potential for identifying SSO in converted-based large-scale energy systems due to their nonlinear nature and the growing number and complexity of measurements being recorded during operation. For future work, a robust noise analysis will be conducted on the synthetic signals, including stochastic analysis (e.g., Monte Carlo simulations) and real noise profiles, to test the method's robustness.

REFERENCES

[1] L. P. Kunjumuhammed, B. C. Pal, C. Oates, and K. J. Dyke, "Electrical oscillations in wind farm systems: Analysis and insight based on detailed modeling," *IEEE Transactions on Sustainable Energy*, vol. 7, pp. 51–62, 1 2016.

[2] I. P. . E. Society, "Wind energy systems sub-synchronous oscillations: Events and modeling," 2020.

[3] Y. Cheng, L. Fan, J. Rose, S. H. Huang, J. Schmall, X. Wang, X. Xie, J. Shair, J. R. Ramamurthy, N. Modi, C. Li, C. Wang, S. Shah, B. Pal, Z. Miao, A. Isaacs, J. Mahseredjian, and J. Zhou, "Real-world subsynchronous oscillation events in power grids with high penetrations of inverter-based resources," *IEEE Transactions on Power Systems*, vol. 38, pp. 316–330, 1 2023.

[4] H. Liu, X. Xie, J. He, T. Xu, Z. Yu, C. Wang, and C. Zhang, "Subsynchronous interaction between direct-drive pmsg based wind farms and weak ac networks," *IEEE Transactions on Power Systems*, vol. 32, pp. 4708–4720, 11 2017.

[5] J. Sun, "Impedance-based stability criterion for grid-connected inverters," *IEEE Transactions on Power Electronics*, vol. 26, pp. 3075–3078, 2011.

[6] B. Badrzadeh, M. Sahni, Y. Zhou, D. Muthumuni, and A. Gole, "General methodology for analysis of sub-synchronous interaction," *IEEE Transactions on Power Systems*, vol. 28, pp. 1858–1869, 2013.

[7] R. N. Damas, Y. Son, M. Yoon, S. Y. Kim, and S. Choi, "Subsynchronous oscillation and advanced analysis: A review," *IEEE Access*, vol. 8, pp. 224 020–224 032, 2020.

[8] C. Karawita, "Hvdc interaction studies using small signal stability assessment," 2019.

[9] Y. Zhan, X. Xie, H. Liu, H. Liu, and Y. Li, "Frequency-domain modal analysis of the oscillatory stability of power systems with high-penetration renewables," *IEEE Transactions on Sustainable Energy*, vol. 10, pp. 1534–1543, 7 2019.

[10] L. Fan, C. Zhu, Z. Miao, and M. Hu, "Modal analysis of a dfig-based wind farm interfaced with a series compensated network," *IEEE Transactions on Energy Conversion*, vol. 26, pp. 1010–1020, 12 2011.

[11] M. Netto and L. Mili, "A robust prony method for power system electromechanical modes identification," 2017.

[12] A. Almunif, L. Fan, and Z. Miao, "A tutorial on data-driven eigenvalue identification: Prony analysis, matrix pencil, and eigensystem realization algorithm," 4 2020.

[13] P. J. Schmid, "Dynamic mode decomposition of numerical and experimental data," *Journal of Fluid Mechanics*, vol. 656, pp. 5–28, 2010.

[14] D. Shu, X. Xie, H. Rao, X. Gao, Q. Jiang, and Y. Huang, "Sub- and super-synchronous interactions between statcoms and weak ac/dc transmissions with series compensations," *IEEE Transactions on Power Electronics*, vol. 33, pp. 7424–7437, 9 2018.

[15] E. Barocio, B. C. Pal, N. F. Thornhill, and A. R. Messina, "A dynamic mode decomposition framework for global power system oscillation analysis," *IEEE Transactions on Power Systems*, vol. 30, pp. 2902–2912, 11 2015.

[16] N. A. S. I. NASPI, "Dynamic system identification toolbox," 2014. [Online]. Available: https://www.naspi.org/node/490

[17] M. Brown, M. Biswal, S. J. Ranade, and H. Cao, "Characterizing and quantifying noise in pmu data," 2016.

[18] S. Wang, J. Zhao, Z. Huang, and R. Diao, "Assessing gaussian assumption of pmu measurement error using field data," *IEEE Transactions on Power Delivery*, vol. 33, pp. 3233–3236, 12 2018.

[19] T. M. Inc., "Signal processing toolbox version: 9.4 (r2024b)," Natick, Massachusetts, United States, 2024. [Online]. Available: https://www.mathworks.com